

Fuel Optimal Trajectory Computation

James W. Burrows*

Boeing Computer Services Company, Seattle, Wash.

Roughly a quarter of the total fuel savings of the new generation of large jet transports will come from the capability of computing fuel optimal flight trajectories between departure point and destination. The shape of the trajectory in the vertical plane is treated here. A simplified mathematical model is described including spline fits to the drag and fuel flow functions. A suboptimal trajectory is found using the maximum principle of optimal control and singular perturbation theory. The inner or boundary-layer solutions are identified as the climb or descent segments of the flight, while the outer solution corresponds to cruise. The inner solutions are expanded to second order in the vicinity of the outer solution to develop cruise control laws for cost-effective response to altered in-flight conditions.

Nomenclature

a	= sound speed, m/s
C_D	= drag coefficient
c_f	= fuel cost, \$/kg
C_L	= lift coefficient
c_t	= time cost, \$/s
D	= drag, N
DOC	= direct operating cost, \$
D_V	= $\partial D(V, E) / \partial V$
D_{VV}	= $\partial^2 D(V, E) / \partial V^2$
D_0	= drag near cruise, N
E	= specific total energy, m
\dot{E}_{com}	= energy rate command, m/s
E_{crz}	= cruise energy, m
EPR	= engine pressure ratio
E_0	= energy near cruise, m
f	= fuel flow rate, kg/s
f_T	= $\partial f / \partial T$
f_{TT}	= $\partial^2 f / \partial T^2$
f_{TV}	= $\partial^2 f(V, E) / \partial T \partial V$
f_V	= $\partial f(V, E) / \partial V$
f_{VV}	= $\partial^2 f(V, E) / \partial V^2$
f_0	= fuel flow rate near cruise, kg/s
g	= gravity acceleration, m/s ²
h	= height or altitude, m
H	= Hamiltonian, \$/s
h_{crz}	= cruise altitude, m
h_0	= altitude near cruise, m
ISA	= 1962 International Standard Atmosphere
K_{CD}	= climb/descent cost function expansion, Eq. (13)
m	= mass, kg
M	= Mach number
S	= reference area, m ²
t	= time, s
T	= thrust, N
T_c	= optimum climb thrust, N
T_d	= optimum descent thrust, N
t_f	= final time, s
T_{max}	= maximum thrust, N
T_{min}	= minimum thrust, N
t_0	= initial time, s
T_0	= thrust near cruise, N
V	= true airspeed, m/s
V_c	= optimum climb speed, m/s
V_{com}	= speed command, m/s
V_{crz}	= cruise speed, m/s

V_d	= optimum descent speed, m/s
V_w	= along-track wind speed, m/s
V_0	= speed near cruise, m/s
x	= range, m
γ	= flight-path angle, rad
ΔD	= $D_V \Delta V + D_{VV} \Delta V^2 / 2$
ΔE	= cruise energy error, m
Δh	= altitude error, m
ΔT	= thrust increment, N
ΔT_{opt}	= optimum thrust increment, N
ΔV	= speed increment, m/s
ΔV_{opt}	= optimum speed increment, m/s
λ_E	= energy adjoint, \$/m
λ_h	= altitude adjoint, \$/m
λ_m	= mass adjoint, \$/kg
λ_x	= range adjoint, \$/m
ρ	= air density, kg/m ³
τ	= cruise feedback time constant, s

Introduction

RECENT fuel price escalation has had a powerful impact on the design and operation of new large civil jet transport aircraft. It is anticipated that improved engine design will produce fuel savings on the order of 10%, while airframe design can save about 5%. A further 5% savings is the goal of improved operational techniques including trajectory optimization.

In a study of fuel optimal trajectories, Schultz and Zagalsky¹ used the maximum principle to derive a ratio which provides speed commands during climb and descent segments, assuming thrust is at its limits. This ratio, which may be called the climb/descent cost function, was derived in a different approach by Barman and Erzberger.² They also showed that a small additional saving is available from variable thrust commands. In this paper, the climb/descent cost function giving both speed and thrust commands is derived from the maximum principle. Changing mass is included as a state variable, and the integration of its adjoint variable proves tractable. Special characteristics of short-haul trajectories² are identified as applications of specific optimal control theory results.

Calise³ used the theory of singular perturbations to derive a ratio which provides speed and altitude commands during cruise, assuming thrust equals drag. An expansion of the climb/descent cost function at cruise was used by Erzberger and Lee⁴ to prove cruise optimality. Their expansion is extended here to the vicinity of cruise to find an approximately optimal cruise feedback control. Finally, simulations are described which show definite, but small, cost savings associated with this control compared to typical linear control during cruise.

Received Dec. 11, 1980; revision received July 13, 1981. Copyright © American Institute of Aeronautics and Astronautics, Inc., 1981. All rights reserved.

*Principal Engineer, Energy Technology Applications Division.

Performance Index and Equations of Motion

The fuel optimal trajectory problem will be treated as a special case of the more general problem of minimizing the direct operating cost (DOC)

$$\int_{t_0}^{t_f} (c_f f + c_t) dt \quad (1)$$

with initial and final times t_0 and t_f , cost of fuel c_f , and fuel flow f . The time cost c_t represents all nonfuel flight costs; the special choice $c_t = 0$ corresponds to the fuel optimal trajectory problem. The final time is assumed to be free.

Neglecting aircraft vertical acceleration and angular motion, and assuming a small flight-path angle γ , the following equations of motion^{1,5} exhibit the major features of optimal flight trajectories.

$$\begin{aligned} \dot{E} &= (T-D)V/mg \\ h &= V\gamma \\ \dot{x} &= V + V_w \\ \dot{m} &= -f \end{aligned} \quad (2)$$

The aircraft mass m is included as a state variable to investigate the special influences of changing mass on cruise. The total energy E per unit weight is given by

$$E = V^2/2g + h \quad (3)$$

With the assumption that the along-track wind V_w changes slowly, the speed V is chosen² to represent true airspeed rather than inertial speed. Other symbols in Eqs. (2) and (3) are thrust T , drag D , gravity $g = 9.80665 \text{ m/s}^2$, height h , and horizontal distance x . The controls are γ and T .

According to the maximum principle of optimal control theory,⁶ the Hamiltonian H is a minimum and equal to zero along an optimal trajectory.

$$\begin{aligned} \min_{T, \gamma} H &= \min \{ c_f f + c_t + \lambda_E (T-D)V/mg + \lambda_h V \\ &\quad + \lambda_x (V + V_w) - \lambda_m f \} = 0 \end{aligned} \quad (4)$$

The adjoint variables λ_E , λ_h , λ_x , and λ_m satisfy the Hamilton-Jacobi equations

$$\begin{aligned} \dot{\lambda}_E &= -\frac{\partial H}{\partial E} \\ \dot{\lambda}_h &= -\frac{\partial H}{\partial h} \\ \dot{\lambda}_x &= -\frac{\partial H}{\partial x} \\ \dot{\lambda}_m &= -\frac{\partial H}{\partial m} \end{aligned} \quad (5)$$

Most of a practical optimal trajectory will be a γ -singular arc¹ along which

$$\lambda_h = 0 = \frac{\partial H}{\partial h} = 0 \quad (6)$$

Equations (4) and (6) combine¹ together with the thrust optimality condition $\partial H/\partial T = 0$ to give an expression for the

energy adjoint variable

$$\begin{aligned} \text{climb} \quad & \begin{cases} D < T \leq T_{\max} \\ (\arg \min = T_c, V_c) \end{cases} \\ & \left[\frac{(c_f - \lambda_m)f + c_t + \lambda_x(V + V_w)}{(T-D)V/mg} \right]_E = -\lambda_E \quad (7) \\ \text{descent} \quad & \begin{cases} T_{\min} \leq T < D \\ (\arg \max = T_d, V_d) \end{cases} \end{aligned}$$

The ratio to be extremized in Eq. (7) has been called the climb/descent cost function and the extremization is to be done at the present value of energy. General initial and final conditions $E(t_0)$, $h(t_0)$, $E(t_f)$, $h(t_f)$ usually involve short initial and terminal nonsingular segments along which Eq. (6) is not satisfied. Such segments will not be treated here, so trajectories will be considered from the beginning of climb to the end of descent.

The initial fuel load is to be determined so that the final mass $m(t_f)$ will be greater than the aircraft zero fuel mass plus a fuel reserve; it may be assumed that the final mass is free and thus $\lambda_m(t_f) = 0$. Backward integration is used to find approximate values of $m(t_0)$ and $\lambda_m(t_0)$.

Aircraft Models

Four quantities in Eqs. (2) and (7) are aircraft dependent: drag $D(E, h, x, m)$, fuel flow $f(E, h, x, T)$, minimum thrust $T_{\min}(E, h, x)$, and maximum thrust $T_{\max}(E, h, x)$. The aircraft modeled in the following example is the Boeing 767, a new 200-passenger, two-engine jet transport presently in the design phase. The estimated drag coefficient $C_D(C_L, M)$ is given as a function of lift coefficient C_L and Mach number M in the form of tabular data. A two-dimensional cubic spline fit⁷ to the drag data was used for two reasons. 1) A smooth drag interpolation method introduces less activity in the climb/descent speed commands V_c, V_d in Eq. (7). 2) The derivatives of drag with respect to speed, available from a spline fit, can be used to improve the search for the optimizing commands in Eq. (7). The latter capability will be used in a later section to find closed loop cruise control. C_L and M are computed from the state variables by

$$C_L = mg / (\frac{1}{2}\rho V^2 S) \quad M = V/a \quad (8)$$

with reference area $S = 283.35 \text{ m}^2$. The first equation of (8) uses the assumption that lift equals weight. The atmospheric parameters air density ρ and sound speed a are functions of meteorological conditions. Such dependence can make the four airplane quantities explicit functions of x . Few studies of the implications of x -variation of wind and temperature have been made; x -variation will be ignored in the following by assuming atmospheric parameters are given by the International Standard Atmosphere (ISA), and V_w is a function of h only. Using the drag coefficient C_D from the spline fit, the drag D is $D = \frac{1}{2}\rho V^2 S C_D$. Figure 1 shows a contour plot of the drag as a function of speed and energy deviations from cruise conditions $V_{crz} = 233.6 \text{ m/s}$ ($M = 0.792$) and $E_{crz} = 15585 \text{ m}$ ($h_{crz} = 12803 \text{ m}$).

Estimated fuel flow was obtained in the form of two tabulations: 1) engine pressure ratio (EPR) as a function of Mach number and corrected net thrust per engine, and 2) corrected fuel flow per engine as a function of EPR and Mach number. Spline fits were made to both of these functions. Figure 2 is a contour plot of fuel flow, assuming thrust is equal to the drag of Fig. 1.

Maximum climb thrust and flight idle thrust were chosen as the upper and lower thrust limits, respectively. Spline fits were made for each of these quantities from tabulations with respect to pressure altitude and Mach number.

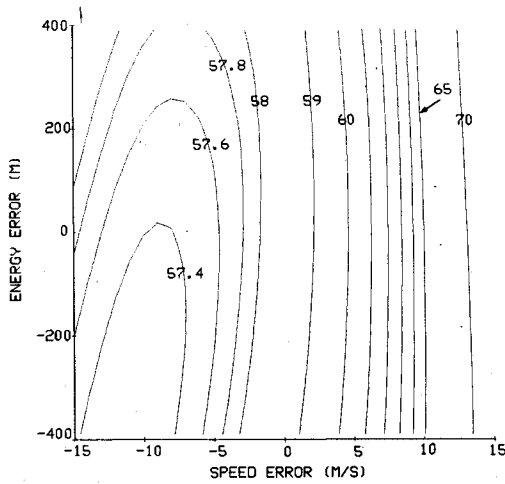


Fig. 1 Estimated B767 drag (kN) in the vicinity of cruise.

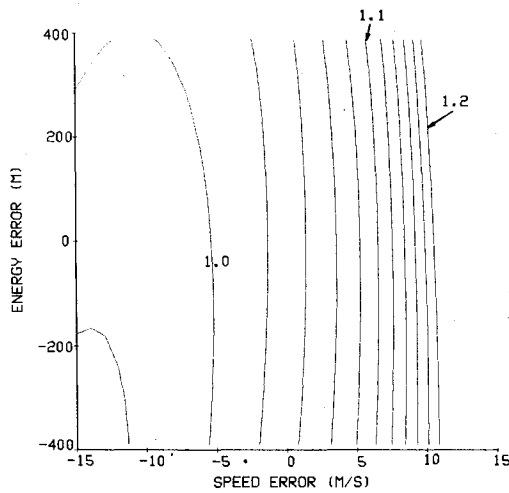


Fig. 2 Estimated B767 fuel flow (kg/s) with thrust = drag.

Optimum Short-Haul Trajectories

During climb, an optimum controller would minimize Eq. (7) over thrust and speed with energy equal to present energy. The minimizing arguments T_c , V_c are thrust and speed commands, and the minimum value of the cost function is the negative energy adjoint $-\lambda_E$. Provisional descent commands T_d , V_d and corresponding energy adjoint are found by maximizing Eq. (7) at present energy. The requirement of adjoint variable continuity along an optimal trajectory implies that a switch from climb to descent can only occur when the two energy adjoint values are equal. The resultant trajectory is short-haul,² with only climb and descent segments. Its range is a function of the choice of λ_x which is a constant under the present assumption $\partial H/\partial x = 0$. Approximate initial values $\lambda_m(t_0)$ were found by backward integration, but the resultant small values of λ_m have little influence on the trajectory.

Figure 3 shows two short-haul trajectories corresponding to the two choices $\lambda_x = -1.13$ and -1.14 \$/km. Points are shown every 100 s along the trajectories. The cost constants are $c_f = 0.154$ \$/kg and $c_t = 0.105$ \$/s, initial mass is 110 Mg, initial and final altitudes are 3 km, initial speed is equal to V_c from Eq. (7) at the initial altitude, and $V_w = 0$. To illustrate the trajectories with simple integration of Eq. (2), the speed change due to flight-path angle change is equal to the speed command $V_{com} = V_c$ or V_d from Eq. (7) with 100 s lag.

$$\gamma = \dot{E}/V - \dot{V}/g = (T - D)/mg - (V_{com} - V)/100g \quad (9)$$

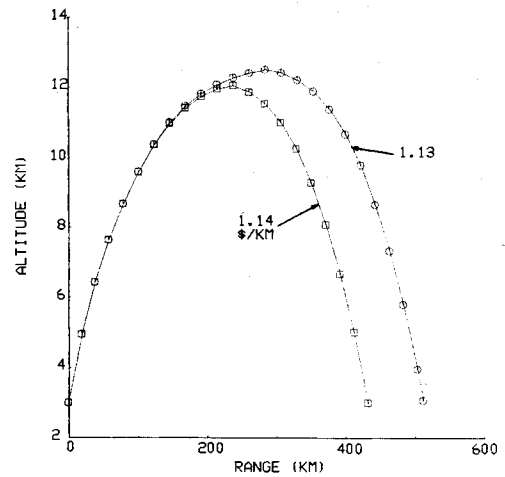
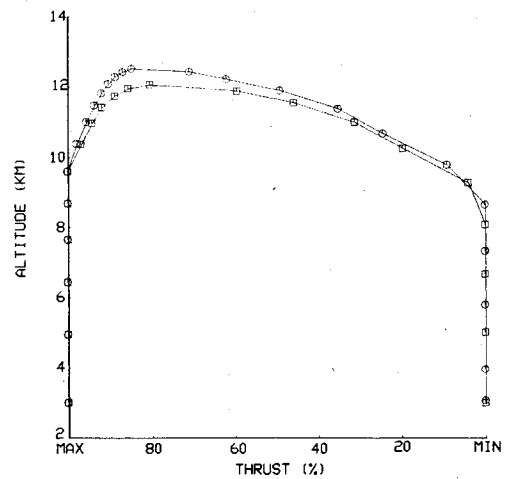
Fig. 3 Two short-haul trajectories with $-\lambda_x = 1.13$ and 1.14 \$/km.

Fig. 4 Ratio of thrust to maximum thrust along short-haul trajectories.

Since V_{com} is the optimum speed, a shorter time constant would result in lower cost, but in practice it could excite unmodeled effects such as elevator drag and vertical accelerations with unknown cost impact. The thrust is equal to T_c or T_d from Eq. (7) and its ratio to maximum thrust is shown in Fig. 4. Partial thrust is used above about 10 km. This saves² about 1.5% of short-haul trajectory cost and is important in the following cruise studies.

Long Range Trajectories

Cruise Cost Function

The full set of equations of motion (2) can be regarded as a singular perturbation³ of the last two equations after setting $T = D$ and $\gamma = 0$. Application of the maximum principle to Eq. (1) and the last two equations of (2) gives

$$\lambda_x = -\min_{E,h} \left[\frac{(c_f - \lambda_m)f(E,h,x,T=D) + c_t}{V + V_w} \right]_m \quad (10)$$

The minimizing arguments are E_{crz} , h_{crz} and the ratio in brackets is called the cruise cost function. This formulation is used in the following implementation to give thrust and speed commands.

1) The minimization in Eq. (10) is performed at intervals throughout the entire trajectory (during climb and descent as well as cruise). h_{crz} will usually slowly increase (cruise climb),

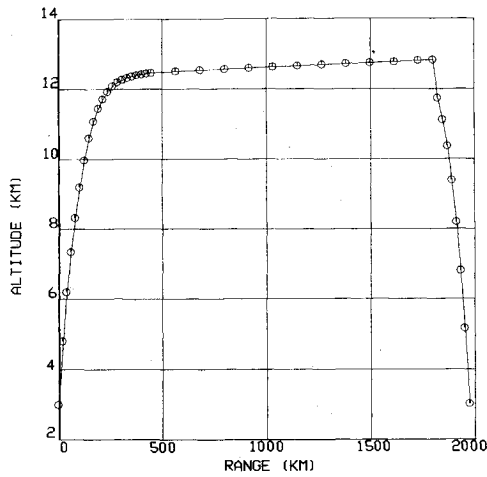


Fig. 5 2000-km DOC-optimal trajectory.

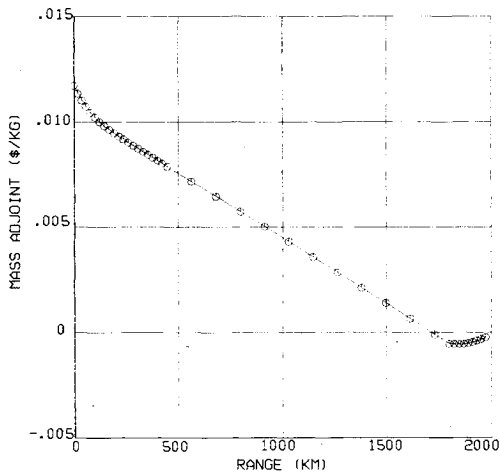


Fig. 6 Mass adjoint variable for long-haul trajectory.

but the value λ_x from Eq. (10) is nearly constant as required by theory. If λ_m were omitted from Eq. (10), as in most past studies in which the mass is treated as a parameter, the value of λ_x would decrease with fuel burn. In the present case, there is little change in h_{crz} , with or without λ_m . However, λ_m does alter DOC-optimal climb and descent speed commands when $c_f \neq 0$. During cruise, thrust and speed commands may be found by simple linear feedback of energy and altitude errors:

$$T = mg(E_{crz} - E) / \tau V_{crz} + D \quad \gamma = (h_{crz} - h) / \tau V_{crz} \quad (11)$$

A more cost effective cruise control is derived in the next section.

2) The value of λ_x from Eq. (10) is used in Eq. (7) during climb and descent, then thrust and speed commands are obtained as for a short-haul trajectory. The short-haul climb/descent switch based on λ_E is not possible; cruise transition occurs when $E = E_{crz}$ and the top of descent point is based on range-to-go.

For the purposes of illustration the choice $\tau = 25$ s was made for the cruise feedback time constant in Eq. (11) and an entire 2000-km trajectory, Fig. 5, was simulated with the above thrust/speed implementation. The mass adjoint variable is shown in Fig. 6, and a speed-altitude plot in Fig. 7.

DOC-Optimal Cruise Control

When altitude or speed errors are encountered during cruise, the climb or descent commands Eq. (7) should be followed until the cruise conditions are regained. The

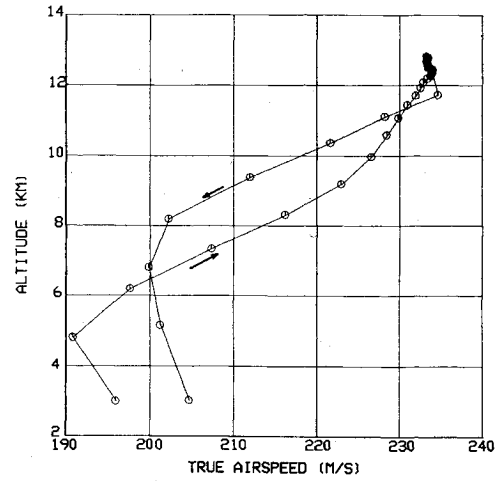


Fig. 7 Long-haul speed-altitude plot.

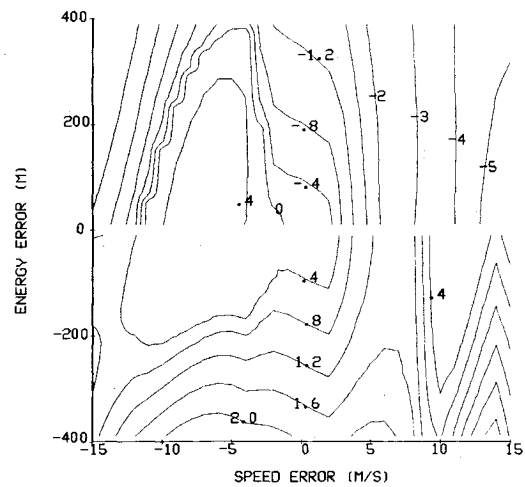


Fig. 8 Contour plot of scaled thrust command (m/s) in vicinity of cruise.

evaluation of Eq. (7) is numerically difficult near cruise because both numerator and denominator are small. Following the methods of singular perturbations, the inner solution³ Eq. (7) is expanded⁴ to second order in incremental thrust and speed in the vicinity of the outer solution Eq. (10). Let E_0, h_0 have values close to E_{crz}, h_{crz} , and define $V_0 = [2g(E_0 - h_0)]^{1/2}$, $T_0 = D_0 = D(E_0, h_0, x, m)$, $f_0 = f(E_0, h_0, x, T_0)$, $\Delta T = T - T_0$, and $\Delta V = V - V_0$. Expanding Eq. (7) gives the incremental thrust and speed commands

$$\Delta T_{opt}, \Delta V_{opt} = \begin{cases} \arg \min \\ \Delta T > \Delta D \\ \Delta V \end{cases} [K_{CD}]_E \quad (12)$$

$$\begin{cases} \arg \max \\ \Delta T < \Delta D \\ \Delta V \end{cases}$$

with

$$K_{CD} = [(c_f - \lambda_m)(f_0 + f_T \Delta T + f_V \Delta V + 1/2 f_{TT} \Delta T^2 + f_{TV} \Delta T \Delta V + 1/2 f_{VV} \Delta V^2) + c_l + \lambda_x (V_0 + V_w + \Delta V)] / [(\Delta T - D_V \Delta V - 1/2 D_{VV} \Delta V^2)(V_0 + \Delta V) / mg] \quad (13)$$

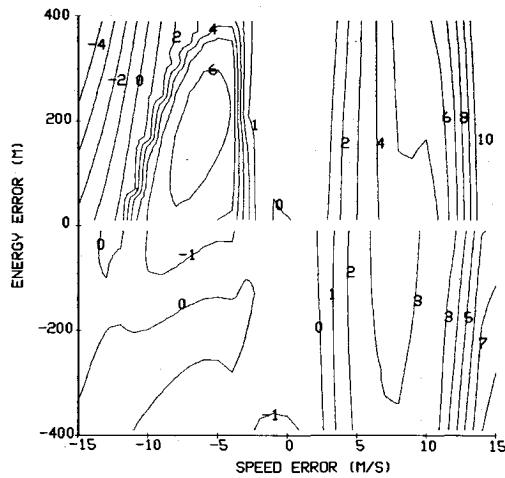


Fig. 9 Contour plot of target speed increment command (m/s) in vicinity of cruise.

where f_T , f_V , D_V , etc., are the derivatives of fuel flow and drag with respect to thrust and speed (at constant energy). The derivative evaluations are facilitated by the spline fits. Considerable simplification occurs if the Mach number is not an explicit function of altitude. This requires the assumption, which is made, that the cruise is in isothermal conditions, e.g., in the stratosphere.

From Eq. (12), the values ΔT_{opt} , ΔV_{opt} are desired at which K_{CD} achieves extreme values. These are found by solving the simultaneous quadratic equations

$$\partial K_{\text{CD}} / \partial (\Delta T) = 0 \quad \partial K_{\text{CD}} / \partial (\Delta V) = 0 \quad (14)$$

There are four or fewer solutions. The sign of the energy error $E_0 - E_{\text{crz}}$ and a second derivative check for maximum (descent) or minimum (climb) are used to choose the correct ΔT_{opt} , ΔV_{opt} pair. Carrying through the above process of finding ΔT_{opt} , ΔV_{opt} for a range of values of ΔE , Δh gives a closed-loop cruise control law. Figure 8 is a contour plot of ΔT_{opt} in the form of an energy rate command $\dot{E}_{\text{com}} = V_{\text{crz}} \Delta T_{\text{opt}} / mg$ with, as before, $V_{\text{crz}} = 233.6$ m/s and $m = 107529$ kg. The control law exhibits a discontinuity across $\Delta E = 0$ and a broad area of slightly positive ΔT_{opt} for speeds slower than cruise. The latter is related to the drag minimum shown in Fig. 1 for the same cruise conditions. For small speed errors, the discontinuity disappears and the feedback is approximately linear in energy with a 200 s time constant. Conventional linear speed error feedback to thrust, with an approximate time constant of 65 s, only occurs for positive speed and energy errors.

Figure 9 is a contour plot of ΔV_{opt} in the form of a change in desired speed $V_0 + \Delta V_{\text{opt}} - V_{\text{crz}}$. The speed commands for ΔE , Δh in the broad area of nearly zero thrust are positive, i.e., decrease altitude to accelerate to speeds slightly higher than V_{crz} . The two conditions that could result in a chattering control (or relaxed cruise⁸), the energy rate discontinuity across $\Delta E = 0$ and a speed increment command equal to speed error, are both present in Figs. 8 and 9, but not at the same point in both figures. Further, any such thrust chattering would be between values less than the thrust limits.

Cruise Control Simulation

Two simulations were run to evaluate the cost savings associated with the DOC-optimal cruise control. The simulations consisted of integrating the equations of motion (2) with various initial off-cruise conditions and with one of two control laws generating T , γ commands. The first control is an approximation to a typical linear control law with speed and altitude error feedback into the thrust and flight-path angle, respectively.

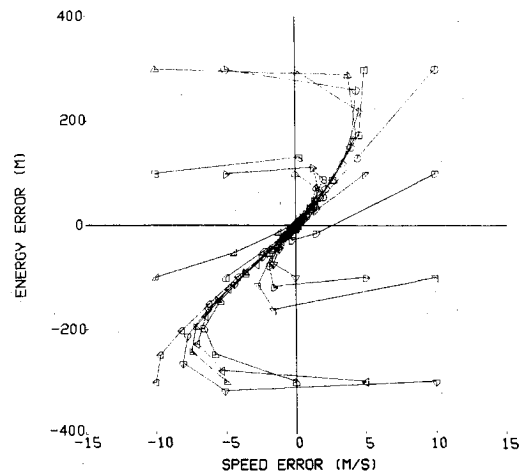


Fig. 10 Cruise capture trajectories with linear control.

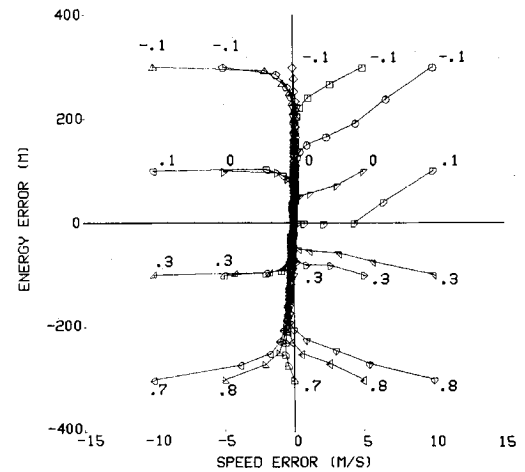


Fig. 11 Cruise capture trajectories with DOC-optimal control. Percent DOC savings during 500 s capture.

$$T = D + m(V_{\text{crz}} - V)/20 \quad \gamma = (h_{\text{crz}} - h)/20V \quad (15)$$

The resultant trajectories starting from twenty different initial conditions are shown in Fig. 10. Points are shown along each trajectory every 50 s. Since the loop time constants are both 20 s, most of the points are close to the origin (corresponding to cruise speed and energy).

The DOC-optimal control was simulated using ΔT_{opt} , ΔV_{opt} from Eq. (12). The speed- γ time constant, unspecified in this theory, was chosen to be 20 s.

$$T = D + \Delta T_{\text{opt}} \quad \gamma = \dot{E}/V - \dot{V}/g = (\Delta T_{\text{opt}}/m - \Delta V_{\text{opt}}/20)/g \quad (16)$$

The resultant trajectories and percent savings compared to linear control during 500 s capture are shown in Fig. 11. Comparing Figs. 10 and 11, the DOC-optimal control law moves the airplane from high and fast initial conditions toward the cruise conditions slower than the linear control law, but costs are nearly the same. From low and slow initial conditions, the DOC-optimal control saves about 0.7%, trading altitude and speed to move the aircraft rapidly toward zero speed error.

A simple explanation of the speed-altitude trade at constant energy to reduce costs can be seen on a contour plot of the cruise cost in Eq. (10) as a function of cruise energy and speed

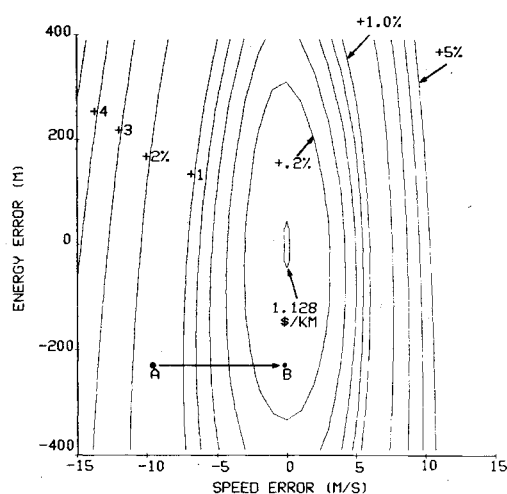


Fig. 12 Contour plot of cruise cost function.

errors (Fig. 12). An aircraft at point A can move to lower cost point B without incremental thrust. The optimal thrust increment to reduce the energy error is given by the climb/descent cost function expansion.

Conclusions

A climb/descent cost function is derived which provides speed and thrust commands for climb and descent. The partial throttle commands, in particular, will save approximately 1.5% of short-haul trip costs.

An expansion of the climb/descent cost function is used to derive optimal speed and thrust commands in the vicinity of the cruise segment of long-haul trajectories. Simulations show that a controller using this closed-loop cruise control will save approximately 0.5% of cruise cost during captures compared to standard autopilot/autothrottle designs.

References

- ¹Schultz, R.L. and Zagalsky, N.R., "Aircraft Performance Optimization," *Journal of Aircraft*, Vol. 9, Feb. 1972, pp. 108-114.
- ²Barman, J.F. and Erzberger, H., "Fixed Range Optimum Trajectories for Short-Haul Aircraft," *Journal of Aircraft*, Vol. 13, Oct. 1976, pp. 748-754.
- ³Calise, A.J., "Extended Energy Management Methods for Flight Performance Optimization," *AIAA Journal*, Vol. 15, March 1977, pp. 314-321.
- ⁴Erzberger, H. and Lee, H., "Constrained Optimal Trajectories with Specified Range," *Journal of Guidance and Control*, Vol. 3, Jan.-Feb. 1980, pp. 78-85.
- ⁵Bryson, A.E., Desai, M.N., and Hoffman, W.C., "Energy-State Approximation in Performance Optimization of Supersonic Aircraft," *Journal of Aircraft*, Vol. 6, Nov.-Dec. 1969, pp. 481-488.
- ⁶Bryson, A.E. and Ho, Y.-C., *Applied Optimal Control*, Blaisdell, New York, 1969, Chap. 3.
- ⁷de Boor, C., "A Practical Guide to Splines," *Applied Mathematical Sciences*, Springer-Verlag, New York, 1978, Vol. 27 Chap. 17.
- ⁸Aggarwal, R. et al., "An Analysis of Fuel Conserving Operational Procedures and Design Modifications for Bomber/Transport Aircraft," AFFDL-TR-78-96, Vol. 2, Appendix B.

From the AIAA Progress in Astronautics and Aeronautics Series . . .

COMBUSTION EXPERIMENTS IN A ZERO-GRAVITY LABORATORY—v. 73

Edited by Thomas H. Cochran, NASA Lewis Research Center

Scientists throughout the world are eagerly awaiting the new opportunities for scientific research that will be available with the advent of the U.S. Space Shuttle. One of the many types of payloads envisioned for placement in earth orbit is a space laboratory which would be carried into space by the Orbiter and equipped for carrying out selected scientific experiments. Testing would be conducted by trained scientist-astronauts on board in cooperation with research scientists on the ground who would have conceived and planned the experiments. The U.S. National Aeronautics and Space Administration (NASA) plans to invite the scientific community on a broad national and international scale to participate in utilizing Spacelab for scientific research. Described in this volume are some of the basic experiments in combustion which are being considered for eventual study in Spacelab. Similar initial planning is underway under NASA sponsorship in other fields—fluid mechanics, materials science, large structures, etc. It is the intention of AIAA, in publishing this volume on combustion-in-zero-gravity, to stimulate, by illustrative example, new thought on kinds of basic experiments which might be usefully performed in the unique environment to be provided by Spacelab, i.e., long-term zero gravity, unimpeded solar radiation, ultra-high vacuum, fast pump-out rates, intense far-ultraviolet radiation, very clear optical conditions, unlimited outside dimensions, etc. It is our hope that the volume will be studied by potential investigators in many fields, not only combustion science, to see what new ideas may emerge in both fundamental and applied science, and to take advantage of the new laboratory possibilities.

280 pp., 6×9, illus., \$20.00 Mem., \$35.00 List

TO ORDER WRITE: Publications Dept., AIAA, 1290 Avenue of the Americas, New York, N.Y. 10104